DOI: 10.31534/engmod.2020.1-2.ri.06f
Professional paper
Received: 1.11.2019.

Mechanism Analysis and Dynamics Simulation of Assist Manipulator

Bao Junhua(1), **He Weidong**(1), **Liao Minghui**(2)

(1) *School of Mechanical Engineering, Dalian Jiao Tong University, Dalian, 116028, CHINA*
e-mail: 20794198@qq.com

(2) *Dalian Tianyun Machinery Co., Ltd., Dalian, 116033, CHINA*

SUMMARY

In order to reduce labour intensity and improve working efficiency, a kind of assist manipulator was designed which is an auxiliary tool used for the assembly line of the marine diesel engine that can conveniently realize the delivery of parts and field assembly. Motion and force analysis of the mechanism of assist manipulator was examined with the help of MATLAB software on the base of d'Alembert principle, the disciplinary of displacement, velocity, acceleration, and force rules in the process of mechanism movement was obtained by mechanical analysis. Based on the kinematical analysis, the parameters of mechanism size were optimized to improve the loading state. The Creo software, ANSYS software, and RecurDyn software were used to model and analyse the rigid-flexible coupling dynamics of the manipulator, and the motion law and stress distribution of the key components was obtained.

KEY WORDS: *assist manipulator; mechanism analysis; multi-body dynamics simulation; rigid-flexible coupling; optimization.*

1. INTRODUCTION

With the rapid development of the world economy, many industries in China have shown the trend of large-scale and industrialized development, and the marine diesel engine industry is no exception. In the power system of a ship, the diesel engine is the core part. In order to improve production efficiency and manufacturing accuracy, it is of great significance to realize the delivery of parts and assist the on-site assembly work and to promote the development of marine diesel engine industrialization [1-2]. To reduce labor intensity and improve labor efficiency, for a certain marine diesel engine assembly production line, a kind of power-assisted manipulator device for auxiliary assembly is designed which can realize the delivery of parts and field installation work. To systematically grasp the working state of the manipulator during the work process [1, 2] the working position and working space of the manipulator are studied, using the coordinate vector variation method combined with the geometric relationship of the mechanism [3, 4]. The motion accuracy, reliability, and sensitivity of the plane linkage mechanism are analyzed and the guidance to the process of manufacture and maintenance [5-6] are given using the momentum exchange method, Hooke's

law, and the finite element method, [3]. Dynamic simulation of a rigid body model and rigid-flexible coupling model of the kinematic system can provide an effective dynamic modeling method and analysis method for the system [7-8]. Based on the previous analysis methods and the specific functional requirements, this paper analyzes the dynamics and virtual simulation of the assembly manipulator. The mechanical analysis and parameter optimization of the parallel rod mechanism that performs the main work in the equipment are performed using MATLAB software. Combining Creo software, ANSYS software, and RecurDyn software modeled the manipulator and simulated the rigid-flex coupling dynamics, which provided a basis for the smooth commissioning and operation of the device [9-10].

The driving device of the assistant manipulator is mainly composed of a parallel six-bar mechanism, guide rail, and other main parts. Each part acts either together or separately under the regulation of the control system to realize the reciprocating movement of the system, forward delivery motion, and the movement of the manipulator resetting and returning. The specific structure of the transmission device is shown in Figure 1. It consists of 8 main parts: 1. parallel six-bar mechanism, 2. guide rail, 3. slider group, 4. parallel suspension device, 5. linear motion module, 6. manipulator arm, 7. mechanical gripper, and 8. arm suspension device.

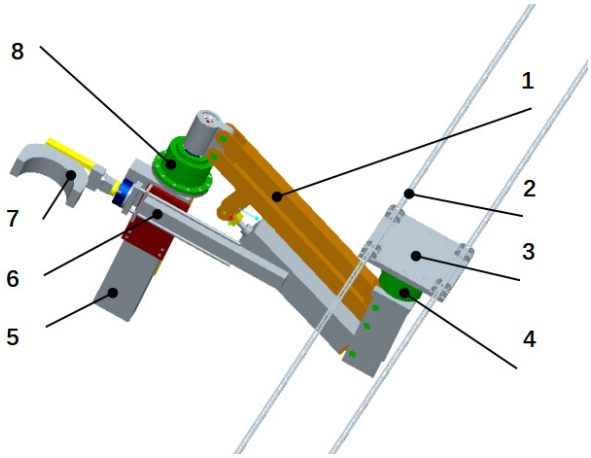

Fig. 1 *Assembly drawing of an assist manipulator*

2. MECHANICS ANALYSIS OF TRANSMISSION SYSTEM

2.1 KINEMATICS ANALYSIS OF TRANSMISSION SYSTEM

To meet the design requirements of the reciprocating movement during the assembly process, a parallel six-bar mechanism for delivering parts of the diesel engine clamped by the manipulators is designed, and the diagram of the mechanism is shown in Figure 2, where link 1 is the driving component. The degree of freedom of the mechanism equals 1, and the mechanism is driven by a pneumatic cylinder composed of link 1 and link 2. The structure consists of six main components: pneumatic linear motion piston 1, pneumatic cylinder block 2, connecting rod 3, connecting rod 4, connecting rod 5, and fixed member 6.

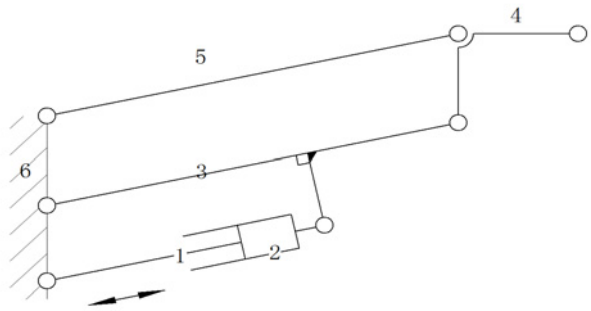

Fig. 2 *Brief drawing of the transmission mechanism*

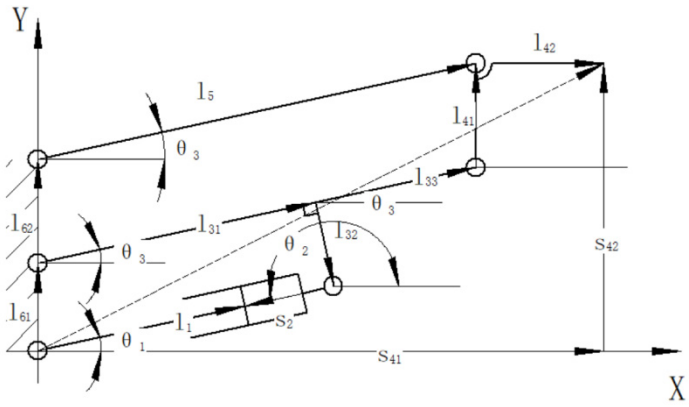

Fig. 3 *Motion vector diagram of the mechanism*

To determine the motion relationship of each component, the mechanism vector diagram is drawn, as shown in Figure 3. The XOY reference coordinate system with the hinge center of link 1 as the coordinate origin is established, and the component vectors (l_i, θ_i) are defined to express the size and direction of the vectors in the coordinate system. According to the relationship among the vectors defined in Figure 3, four sets of vector equations are determined. See Formula 1a:

$$\begin{Bmatrix} \overrightarrow{l_{61}} + \overrightarrow{l_{31}} + \overrightarrow{l_{32}} + \overrightarrow{s_2} = \overrightarrow{l_1} \\ \overrightarrow{l_{62}} + \overrightarrow{l_5} = \overrightarrow{l_{31}} + \overrightarrow{l_{33}} + \overrightarrow{l_{41}} \\ \overrightarrow{l_{61}} + \overrightarrow{l_{62}} + \overrightarrow{l_5} + \overrightarrow{l_{42}} = \overrightarrow{s_{41}} + \overrightarrow{s_{42}} \end{Bmatrix} \quad \textbf{(1a)}$$

The vector relation is projected to *X* and *Y* axes, and the vector equation is transformed into a set of scalar equations. See Formula 1b:

$$\begin{gathered} l_{31}\cos\theta_3 + l_{32}\sin\theta_3 = (s_2 + l_1)\cos\theta_1 \\ l_{61} + l_{31}\sin\theta_3 - l_{32}\cos\theta_3 = (s_2 + l_1)\sin\theta_1 \\ l_5\cos\theta_3 + l_{42} = s_{41} \\ l_6 + l_5\sin\theta_3 = s_{42} \end{gathered} \quad \textbf{(1b)}$$

Among them:

l_i - The length of links,

θ_i - Rotation angles of components,

s_i - Centroid displacement of the corresponding components.

Through the vector equation, the scalar equation system and its matrix form of the mechanism are written out. Formula 1b is derived once and the velocity equations of the mechanism are obtained. The matrix equations are expressed in Formula 2:

$$\begin{bmatrix} l_{32}\cos\theta_3 - l_{31}\sin\theta_3 & (s_2+l_1)\sin\theta_1 & 0 & 0 \\ l_{31}\cos\theta_3 + l_{32}\sin\theta_3 & -(s_2+l_1)\cos\theta_1 & 0 & 0 \\ l_5\sin\theta_3 & 0 & 1 & 0 \\ -l_5\cos\theta_3 & 0 & 0 & 1 \end{bmatrix} \begin{bmatrix} \omega_3 \\ \omega_1 \\ v_{41} \\ v_{42} \end{bmatrix} = \begin{bmatrix} -v_2\cos\theta_1 \\ v_2\sin\theta_1 \\ 0 \\ 0 \end{bmatrix} \quad (2)$$

Among them:

v_{ij} - The velocity of the center of mass of link 4,

ω_i - Angular velocity of link i.

The acceleration equations of the mechanism are obtained by calculating the first derivative of the velocity equations. The matrix equation can be expressed as in Formula 3:

$$\begin{bmatrix} l_{32}\cos\theta_3 - l_{31}\sin\theta_3 & (s_2+l_1)\sin\theta_1 & 0 & 0 \\ l_{31}\cos\theta_3 + l_{32}\sin\theta_3 & -(s_2+l_1)\cos\theta_1 & 0 & 0 \\ l_5\sin\theta_3 & 0 & 1 & 0 \\ -l_5\cos\theta_3 & 0 & 0 & 1 \end{bmatrix} \begin{bmatrix} \varepsilon_3 \\ \varepsilon_1 \\ a_{41} \\ a_{42} \end{bmatrix}$$

$$= \begin{bmatrix} (l_{32}\sin\theta_3 + l_{31}\cos\theta_3)\omega_3^2 - ((s_2+l_1)\cos\theta_1)\omega_1^2 \\ (l_{31}\sin\theta_3 - l_{32}\cos\theta_3)\omega_3^2 - ((s_2+l_1)\sin\theta_1)\omega_1^2 + 2\cos\theta_1\cdot\omega_1\cdot v_2 \\ -l_5\cos\theta_3\cdot\omega_3^2 \\ -l_5\sin\theta_3\cdot\omega_3^2 \end{bmatrix} \quad (3)$$

Among them:

a_{ij} - the acceleration of the center of mass of link 4,

ε_i - Angular acceleration of link i.

2.2 MOTION ANALYSIS AND SOLUTION

Firstly, the displacement of the mechanism is solved, and the program solution is carried out using the software system of MATLAB through the preparation of *.m documents [11-12]. According to formula (1b), the position coordinate equation is written as a 'Function', and then to solve it, the solution is called. In order to realize the lifting motion of the parts and save operation space, the motion range of link 3 of the connecting rod is adjusted to swing $30°$ above and below the horizontal position during the actual movement of the mechanism. The rotation angle θ_3 of link 3 is taken as the independent variable for solving the rotation angle θ_1 of the piston rod link 1, and the *X*-direction displacement s_{41} and *Y*-direction displacement s_{42} of the centroid point *K* of link 4 of the connecting rod. By programming solution, the

variation law of the rotation angle and the displacement of the link's center of mass are obtained, as shown in Figure 4.

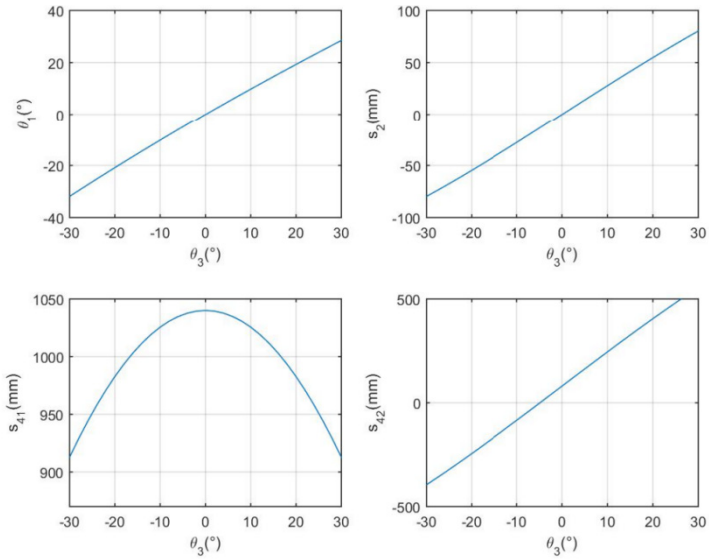

Fig. 4 *Curves of rotation angle and centroid displacement of the main components of the mechanism*

According to the calculation results, the range of rotation angle θ_1 of link 1 is *-31.885°-28.487°*, the range of travel of the piston is *-79.65-80.28 mm*, and the total travel is *159.93 mm*.

According to the results of the analysis and calculation, a pneumatic cylinder product with a suitable structure size can be selected as the mechanism driving part.

The velocity equation (2) is solved. The relative velocity of the cylinder 2 is v_2*=20mm/s* as a known condition. As independent variables, the angular velocity ω_1 of the piston rod of link 1, the angular velocity ω_3 of link 3, *K*-point *X*-direction velocity v_{41}, and *Y*-direction velocity v_{42} of the connecting rod of link 4 are solved. The velocity variation law of each component is shown in Figure 5.

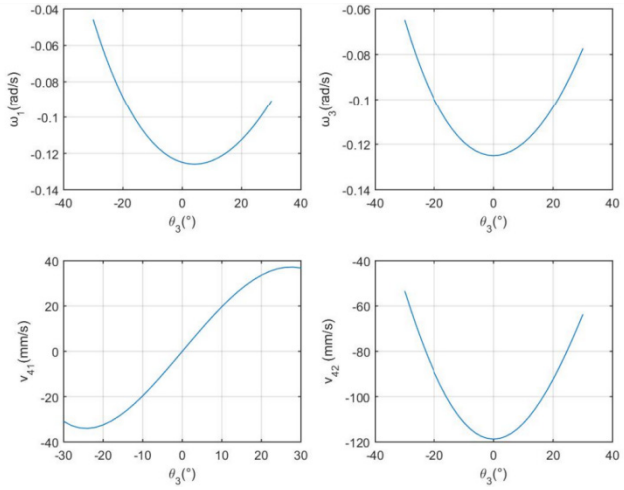

Fig. 5 *Angular velocity of the actuating component and velocity curve of the component centroid*

The acceleration equation (3) is solved by programming. The relative moving speed of cylinder link 2 is v_2=20mm/s. As an independent variable, the angular acceleration ε_1 of the piston rod, the angular acceleration ε_3 of link 3, *K*-point *X*-direction acceleration α_{41} and *Y*-direction acceleration α_{42} of the connecting rod are solved. The acceleration variation of each component is shown in Figure 6.

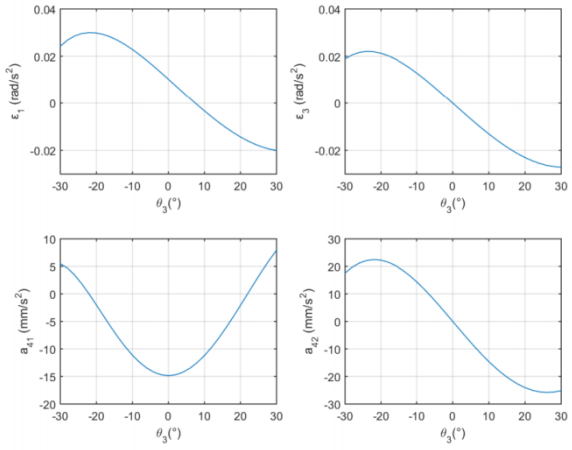

Fig. 6 *Angular acceleration of the actuator and acceleration curve of the centroid*

3. FORCE ANALYSIS AND DIMENSION OPTIMIZATION OF MECHANISMS

3.1 FORCE ANALYSIS

During the working process of the mechanism, the resistance load is expressed by F_r, and the magnitude of the load is *800 N*. This load is the resultant force of the lifting weight and inertia force, and acts on the centroid *K* point of link 4, as shown in Figure 7 (a). The driving force of the mechanism is the working pressure P_2 acting on the piston of the pneumatic cylinder. According to the size of the mechanism, it is necessary to calculate the required cylinder working pressure according to F_r, in order to select the appropriate pneumatic driving device. Therefore, the force analysis and solution calculation of the mechanism are carried out.

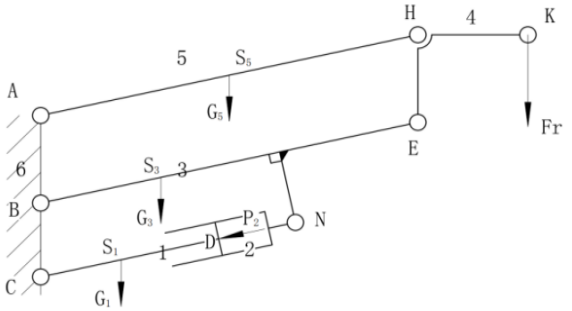

(a) Force diagram of the mechanism

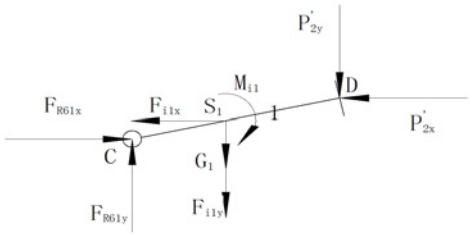

(b) Force diagram of link 1

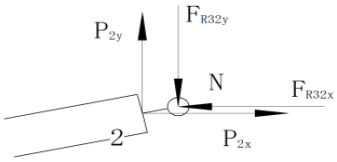

(c) Force diagram of link 2

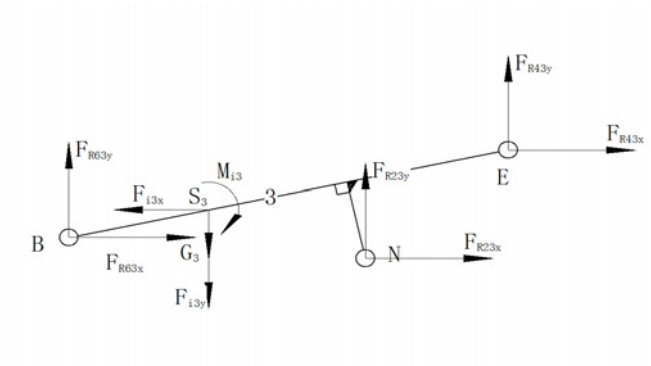

(d) Force diagram of link 3

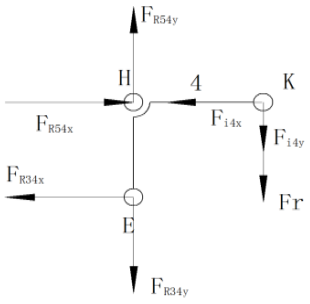

(e) Force diagram of link 4

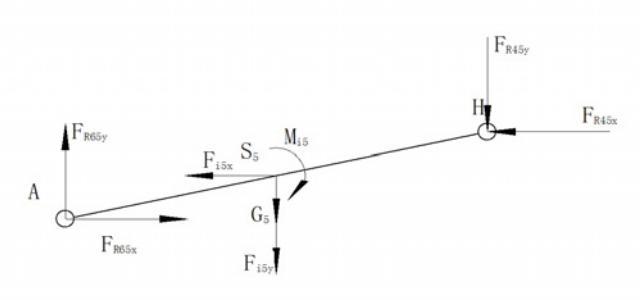

(f) Force diagram of link 5

Fig. 7 *Force analysis diagram of the mechanism and components*

The force analysis of each component is carried out, and the force state is shown in Figure 7. The positive directions of each force are defined as *X* and *Y* axes, and each moment is counterclockwise in a positive direction. The force and moment balance equations of each component are listed below.

According to the D'Alambert principle, list the equilibrium equations of link 1.

$$\sum F_x = 0 : -P'_{2x} + F_{R61x} - F_{i1x} = 0$$

$$\sum F_y = 0 : -P'_{2y} + F_{R61y} - F_{i1y} - G_1 = 0$$

$$\sum M_C = 0 : -P'_{2x}(y_C - y_D) - P'_{2y}(x_D - x_C) - F_{i1x}(y_C - y_{S_1}) - F_{i1y}(x_{S_1} - x_C) - G_1(x_{S_1} - x_C) - M_{i1} = 0$$

where:

Normal acceleration of the center of mass: $a^n_{S_1} = \omega_1^2\left(\frac{l_1}{2}\right)$;

Tangential acceleration of the center of mass: $a^\tau_{S_1} = \varepsilon_1\left(\frac{l_1}{2}\right)$;

The acceleration of the center of mass in the XOY coordinate system can be expressed with the above two accelerations.

$$a^x_{S_1} = -a^n_{S_1}\cos\theta_1 - a^\tau_{S_1}\sin\theta_1$$

$$a^y_{S_1} = -a^n_{S_1}\sin\theta_1 + a^\tau_{S_1}\cos\theta_1$$

The inertia force is positive in the negative direction of X and Y axes:

$$F_{i1x} = m_1 a^x_{S_1}$$

$$F_{i1y} = m_1 a^y_{S_1}$$

The moment of inertia is positive in clockwise direction:

$$M_{i1} = J_{S_1}\varepsilon_1 = m_1\left(\frac{l_1}{2}\right)^2\varepsilon_1$$

The force analysis is carried out for link 2, and the reaction force of link i to link j on the joint is used to represent as F_{Rij}, and the force diagram is as shown in the Figure 7(c).

$$\sum F_x = 0 : P_{2x} - F_{R32x} = 0$$
$$\sum F_y = 0 : P_{2y} - F_{R32y} = 0$$

where:

$$P_{2x} = P'_{2x}$$
$$P_{2y} = P'_{2y}$$

The force analysis of link 3 is as shown in the Figure 7(d).

$$\sum F_x = 0 : F_{R63x} + F_{R23x} + F_{R43x} - F_{i3x} = 0$$
$$\sum F_y = 0 : F_{R63y} + F_{R23y} + F_{R43y} - F_{i3y} - G_3 = 0$$
$$\sum M_B = 0 : F_{R43x}(y_B - y_E) + F_{R43y}(x_E - x_B) + F_{R23x}(y_B - y_N) + F_{R23y}(x_N - x_B)$$
$$-F_{i3x}(y_B - y_{S_3}) - F_{i3y}(x_{S_3} - x_B) - G_3(x_{S_3} - x_B) - M_{i3} = 0$$

where:

$$a_{S_3}^n = \omega_3^2\left(\frac{l_5}{2} - 0.05\right)$$
$$a_{S_3}^\tau = \varepsilon_3\left(\frac{l_5}{2} - 0.05\right)$$
$$a_{S_3}^x = -a_{S_3}^n \cos\theta_3 - a_{S_3}^\tau \sin\theta_3$$
$$a_{S_3}^y = -a_{S_3}^n \sin\theta_3 + a_{S_3}^\tau \cos\theta_3$$
$$F_{i3x} = m_3 a_{S_3}^x$$
$$F_{i3y} = m_3 a_{S_3}^y$$
$$M_{i3} = J_{S_3}\varepsilon_3 = m_3\left(\frac{l_5}{2} - 0.05\right)^2 \varepsilon_3$$

The force analysis of link 4 is as shown in the Figure 7(e).

$$\sum F_x = 0 : -F_{R34x} + F_{R54x} - F_{i4x} = 0$$
$$\sum F_y = 0 : F_{R54y} - F_{R34y} - F_{i4y} - F_r = 0$$
$$\sum M_H = 0 : -F_{R34x}(y_H - y_E) - F_{i4y}(x_K - x_H) - F_r(x_K - x_H) = 0$$

where:

$$F_{i4x} = m_4 a_{S_4}^x$$
$$F_{i4y} = m_4 a_{S_4}^y$$

The force analysis of link 5 is as shown in the Figure 7(f).

$$\sum F_x = 0 : F_{R65x} - F_{R45x} - F_{i5x} = 0$$
$$\sum F_y = 0 : F_{R65y} - F_{R45y} - F_{i5y} - G_5 = 0$$

$$\sum M_A = 0 : -F_{R45x}(y_A - y_H) - F_{R45y}(x_H - x_A)$$
$$-F_{i5x}(y_A - y_{S_5}) - F_{i5y}(x_{S_5} - x_A) - G_5(x_{S_5} - x_A) - M_{i5} = 0$$

where:

$$a_{S_5}^n = \omega_5^2\left(\frac{l_5}{2}\right)$$

$$a_{S_5}^\tau = \varepsilon_5\left(\frac{l_5}{2}\right)$$

$$a_{S_5}^x = -a_{S_5}^n \cos\theta_5 - a_{S_5}^\tau \sin\theta_5$$

$$a_{S_5}^y = -a_{S_5}^n \sin\theta_5 + a_{S_5}^\tau \cos\theta_5$$

$$F_{i5x} = m_5 a_{S_5}^x$$

$$F_{i5y} = m_5 a_{S_5}^y$$

$$M_{i5} = J_{S_5}\varepsilon_5 = m_5\left(\frac{l_5}{2}\right)^2 \varepsilon_5$$

According to the result of the force analysis, the matrix method is used to solve the problem. The matrix equation is Formula 4.

$$\begin{bmatrix} -1 & 0 & & & & & & & & & & & & & & \\ 0 & -1 & & & & & & & & & & & & & & \\ y_D - y_C & x_C - x_D & & & & & & & & & & & & & & \\ & & \ddots & & & & & & & & & & & & & \\ & & & \ddots & & & & & & & & & & & & \\ & & & & \ddots & & & & & & & & & & & \\ & & & & & \ddots & & & & & & & & & & \\ & & & & & & \ddots & & & & & & & & & \\ & & & & & & & & & & & & & & & \\ & & & & & & & & & & & & & & & \\ & & & & & & & & & & & & & & & \\ & & & & & & & & & & & & & & & \\ & & & & & & & & & & & & & & & \\ & & & & & & & & & & & & & & & \\ & & & & & & & & & & & & & & & \\ & & & & & & & & & & & & 0 & 1 & 0 & \\ & & & & & & & & & & & & -1 & 0 & 1 & \\ & & & & & & & & & & & & x_A - x_H & 0 & 0 & \end{bmatrix} \begin{bmatrix} p_{2x} \\ p_{2y} \\ F_{R61x} \\ F_{R61y} \\ F_{R23x} \\ F_{R23y} \\ F_{R43x} \\ F_{R43y} \\ F_{R63x} \\ F_{R63y} \\ F_{R54x} \\ F_{R54y} \\ F_{R65x} \\ F_{R65y} \end{bmatrix} = \begin{bmatrix} F_{i1x} \\ F_{i1y} \\ \cdot \\ \cdot \\ \\ \\ \\ \\ \\ \\ \cdot \\ \cdot \\ F_{i5x} \\ F_{i5x} \cdots \end{bmatrix} \quad \textbf{(4)}$$

By solving the matrix equation of force in MATLAB, the magnitude and direction of reaction force can be obtained. When the mass and inertia force of the components are not considered, the required axial force of the cylinder is obtained, as shown in Figure 8 (a). The maximum working load of the cylinder is *4844.5 N* during the up-swing of the quadrilateral mechanism.

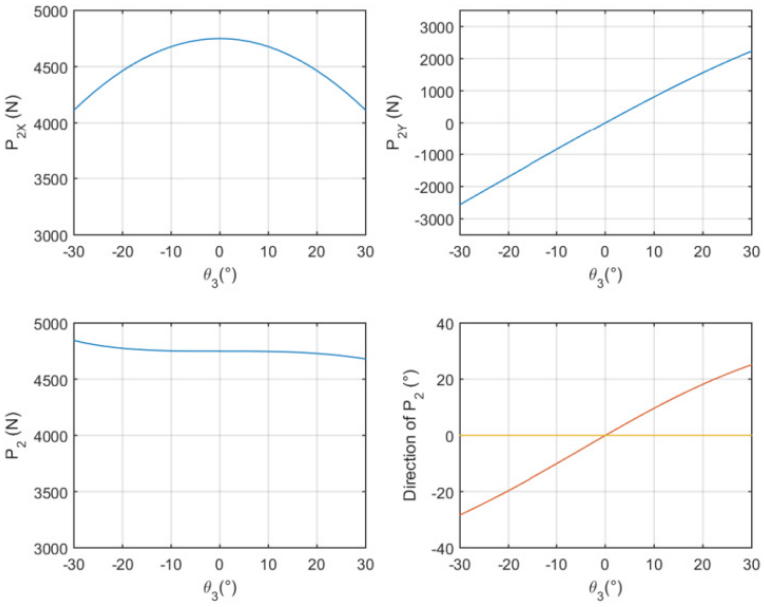

(a) Mass and inertia load not recorded

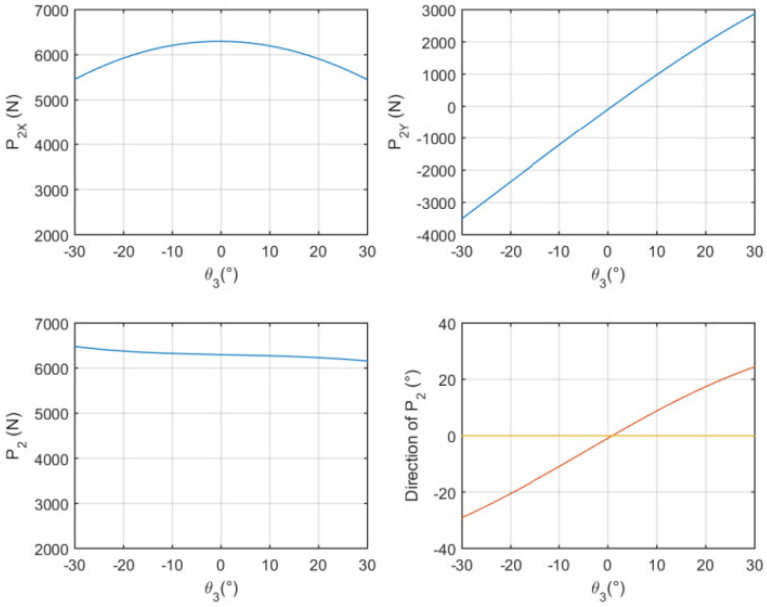

(b) Considering mass and inertia load

Fig. 8 *Driving force curve of the driving cylinder*

Considering the inertia forces, the driving force of the cylinder under the same load condition is shown in Figure 8 (b). Because of the interaction of components' gravity and inertia force, the required driving force of the cylinder is *6473.6 N*, which is *25.2%* higher than that calculated without these considerations. It shows that the quality of components has a greater impact on driving force, and it is necessary to minimize component quality if the condition is to guarantee strength and stiffness.

3.2 STRUCTURAL PARAMETER OPTIMIZATION

3.2.1 PARAMETER DESIGN STUDY

The structure of the manipulator is a six-bar mechanism, and its main structure size and component quality are determined by the component length. Therefore, the purpose of this optimization is to obtain the optimal length combination which can minimize the driving load of the mechanism in the working process. Therefore, the sensitivity analysis of the length of each component affecting the driving force is carried out first to obtain a reasonable range of optimum design parameters. The sensitivity analysis shows that the magnitude of the driving force is mainly affected by length l_{31}=*732mm*, l_{32}=*160mm*, and l_5=*950*; and the quality of links is m_3=*20.8 kg*, m_5=*19.4 kg*, of which l_{32} and l_5 are the most significant, as shown in Figure 9.

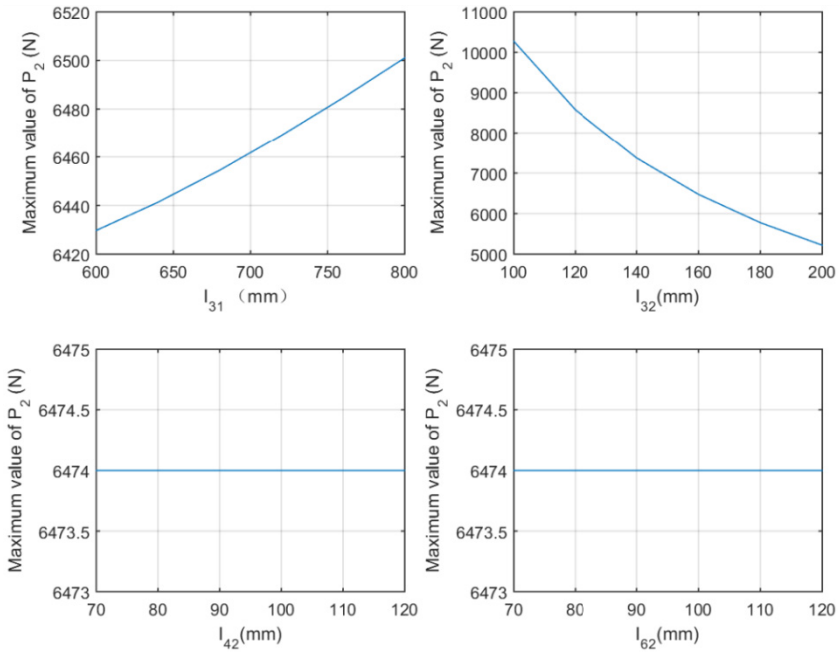

(a)

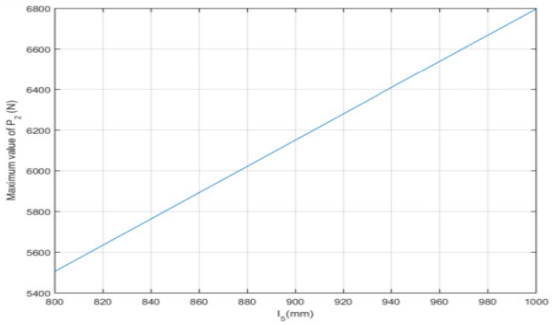

(b)

Fig. 9 *Driving force curve of cylinder influenced by component size*

3.2.2 OPTIMUM DESIGN OF PARAMETERS

According to the results of sensitivity optimization, the optimization parameters and the length range are l_{31}[*600, 800*], l_{32}[*100, 200*] and l_5[*800, 1000*], and appropriate optimization intervals are set as equality constraints to solve the optimization problem. According to the requirement of mechanical performance, the driving axial force P_2 acting on the cylinder block is taken as the objective function. That is: *Minf* (x) = P_2. This statement creates an optimization options structure called options in which the display parameter is set to 'iter' and the TolFun parameter is set to 1e-8.

In this paper, the constrained nonlinear multivariate optimization command 'Fmincon' in the optimization toolbox of MATLAB is used to solve the optimization problem of the structure. The objective function to be solved in optimization is a solution of a non-linear implicit equation system determined by the size and load of the component. By calling the force analysis program, the optimal calculation results of this case are obtained in the feasible region: $\boldsymbol{X}$=[l_{31}, l_{32}, l_5]=[*600*, *200*, *800*], and the maximum driving force of the optimized cylinder is P_2=*4410 N*, which is *31.9%* lower than that before optimization. It has an obvious effect and can efficaciously improve the force state of the whole transmission system.

4. STRUCTURAL MODELING AND SYSTEM RIGID-FLEXIBLE COUPLING DYNAMICS SIMULATION ANALYSIS

Firstly, the three-dimensional solid assembly model of the booster manipulator is established in Creo software system, and the necessary structure is simplified. Save as *.x_t file format serves as the basis for subsequent dynamic model modeling.

RecurDyn software system is a new generation of multi-body system dynamics simulation software. It adopts the relative coordinate system motion equation theory and the complete recursive algorithm and is very suitable for solving large-scale and complex contact multi-body system dynamics problems. In this paper, the sub-model modeling method is used to build subsystem models step by step [8]. Modeling and dynamic debugging modes including parallel mechanism suspension subsystem, parallel mechanism, vertical lifting mechanism, arm telescopic mechanism, wrist and claw mechanism are completed respectively. Finally, the overall assembly modeling is completed, and the dynamic model is shown in Figure 10.

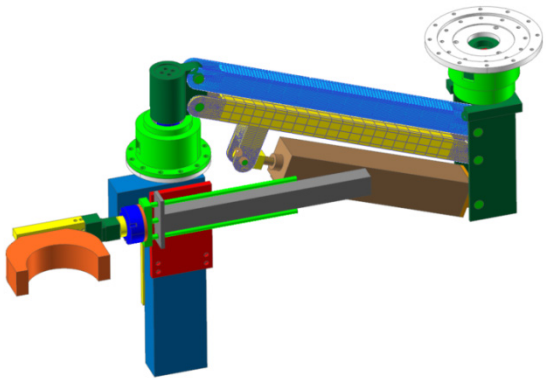

Fig. 10 *System dynamics model*

To obtain the stress change of the specific parts in the working process and to understand and check their strength, the rigid-flexible coupling model of the parallel mechanism sub-model studied in the previous section is adopted, and its rigid-flexible coupling subsystem model is established. Link 3 and link 5 of the connecting rod are introduced into the ANSYS software for the finite element flexibility processing. Through the simulation analysis of the rigid-flexible coupling model, the stress changes of the two main stressed components are dynamically understood to ensure the safe operation of the equipment. The original dimension parameters are used to model and simulate the model size. The moving speed of *20 mm/s* is set on component link 1 to drive parallel mechanism.

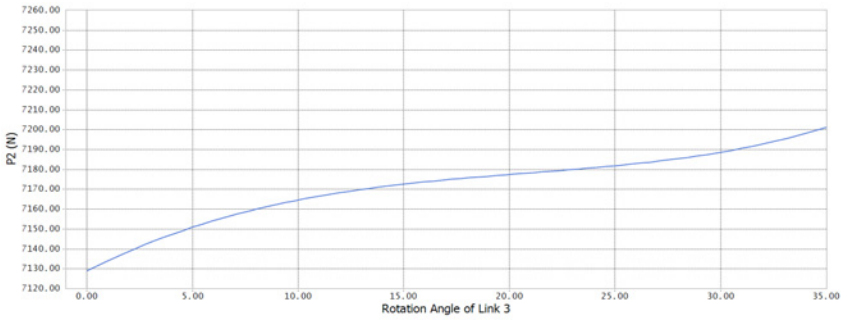

Fig. 11 *Variation curve of the axial driving force of the cylinder*

The driving force acting on the cylinder is *7214 N* according to simulation analysis, which is a *10%* deviation from the calculation results obtained by dynamic analysis of the mechanism. Through simulation analysis, the stress level of component link 3 is relatively high, with a maximum of about *150 Mpa*. The stress concentration is on the hinge position of the two rotating pairs. The stress distribution is shown in Figure 12.

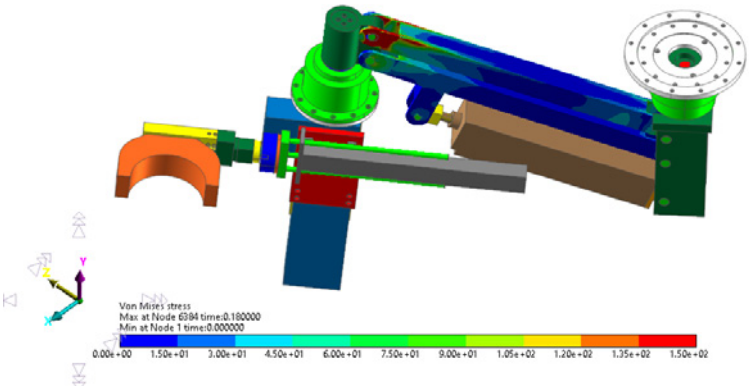

Fig. 12 *Stress distribution*

5. CONCLUSION

Through the system analysis and Simulation of the auxiliary assembly manipulator equipment used in a marine diesel engine assembly line, this paper completes the mechanical analysis and force analysis of the equipment, and completes the optimization design of structural parameters. Combining with the software of MATLAB, the parallel bar mechanism, which is the main working construction in the equipment, is analyzed; the law of displacement, velocity,

and acceleration change in the process of mechanism working is obtained; the range of driving force and then suitable driving equipment of the driving device required for its normal operation are also obtained. By optimizing the size of the mechanism, a better structure size was obtained to reduce the size of the structure and optimize the parameters of the driving device. The driving force is reduced from *6473.6 N* to *4410 N*, which is *31.9%* lower than that before optimization, and satisfactory results are obtained. The modeling and dynamic simulation analysis of the manipulator are carried out combining Creo software and RecurDyn software. The motion and dynamic parameters more in line with the actual working state are determined under the condition of considering the concrete structure, size, and quality of the component. The rigid-flexible coupling model of the system is set up, analyzed, and simulated with the finite element ANSYS software system, and the stress distribution of the main bearing components is obtained. The maximum stress is *150 Mpa* on the joint of link 4. The stress distribution of the main bearing components is obtained for the reason of safety and reliability. The theoretical basis is provided with the use of equipment.

6. ACKNOWLEDGEMENT

This work was support by the Department of Education of Liaoning Province, China. (No. JDL2019002) and the Ministry of Science and Technology of China. (No.2017YFB300700) Thanks for their support.

7. REFERENCE

[1] J. Cheng, J.X. Wang, H.P. Zhu, Current situation of marine diesel engine industry in China, *Guangdong Shipbuilding*, Vol. 34, No. 4, pp. 21-24, 2014.

[2] X.Y. Lu, G. Hou, H.L. Bai, F. Liu, R.H. Cheng, Exploration on the device of robot hand for easy and convenient apple picking, *Grain Science and Technology and Economy*, Vol. 43, No. 9, pp. 93-94, 2018.

[3] Z.L. Zhang, Z.L. Jin, J.Z. Zhang, Workspace analysis of a novel feeding manipulator, *China Mechanical Engineering*, Vol. 27, No. 13, pp. 1743-1747, 2016.

[4] Y.R. Xian, Research and design of automatic feeding manipulator, *Mechanical and Electrical Engineering Technology*, No. 8, pp. 95-96+176, 2019.

[5] H. Pang, T.X. Yu, B.F. Song, Analysis of kinematic accuracy reliability and sensitivity for a planar linkages mechanism, *China Mechanical Engineering*, Vol. 25, No. 18, pp. 2415-2421, 2014.

[6] L.B. Hang, Y. Wang, T.L. Yang, Analysis of a new type 3 translations -1 rotation decoupled parallel manipulator, *China Mechanical Engineering*, Vol. 25, No. 12, pp. 3-5+9, 2004.

[7] Y. Zhao, C.M. Ruan, S.W. Wang, Second-order accurate modeling and experimental studies of rigid-flexible coupled flexible manipulator, *China Mechanical Engineering*, Vol. 29, No. 2, pp. 205-210, 2018.

[8] X.W. Zhang, RecurDyn multi-body system optimization simulation technology, Beijing: Tsinghua University Press, 2010.

[9] Dingyü Xue, OptimFOPID: A MATLAB Interface for Optimum Fractional-Order PID Controller Design For Linear Fractional-Order Plants[C], Hohai University.Program of

the Fifth Symposium on Fractional Differentiation and Its Applications. Hohai University: Chinese society of mechanics, pp. 113, 2012.

[10] Akhil Kadiyala, Devinder Kaur, Ashok Kumar, Application of MATLAB to select an optimum performing genetic algorithm for predicting in-vehicle pollutant concentrations[J], *Environmental Progress & Sustainable Energy*, Vol. 29, pp. 398-405, 2010. https://doi.org/10.1002/ep.10527

[11] Halil Dikbas, Semih Taskaya, Alloying the surface of AISI 2205 duplex stainless steel material by PTA welding method and making its thermomechanical investigation in ANSYS software[J], *Journal of Thermal Analysis and Calorimetry*: An International Forum for Thermal Studies, Vol. 139, pp. 3847-3856, 2020.

https://doi.org/10.1007/s10973-019-09204-6

[12] Alexander Busch, Stein Tore Johansen, On the validity of the two-fluid-KTGF approach for dense gravity-driven granular flows as implemented in ANSYS Fluent R17.2[J], *Powder Technology*, Vol. 364, pp. 429-456, 2020.

https://doi.org/10.1016/j.powtec.2020.01.043